Asymmetric Flexible Strategies Enable Liquid Crystalline Transitions During Thermal Annealing of the Device in Organic Solar Cells

Dong Han,[a1] Minggeng Ding,[a1] Bin Tang,[b] Kai Song,[a] Jing Lv,[a] Xichang Bao*[bc] and Mingliang Sun*[a]

[a] *School of Materials Science and Engineering, Ocean University of China, Qingdao 266100, China*

[b] *Qingdao Institute of Bioenergy and Bioprocess Technology, Chinese Academy of Sciences, Qingdao 266101, China*

[c] *Laboratory of Solar Energy, Shandong Energy Institute, Qingdao 266101, China*

[1] *These authors contributed equally: Dong Han, Minggeng Ding.*

[*] *Corresponding authors. E-mail: baoxc@qibebt.ac.cn (X. Bao), mlsun@ouc.edu.cn (M. Sun).*

Materials

Common solvents were dried and purified by standard procedures. Column chromatography characterizations were performed with the use of silica gel (200-300 mesh). Other reagents were purchased from commercial sources and used directly unless otherwise noted.

Characterization

^{1}H NMR and ^{13}C NMR spectra were recorded using a Bruker AVANCE-III 600 spectrometer with tetramethylsilane (TMS) as an internal standard. TGA and DSC were performed on a Mettler TGA/DSC2/1600HT simultaneous thermal analyzer. UV-vis absorption spectra were obtained on a UV−vis 2550 spectrophotometer. All film samples were spin-casted on quartz glass substrates. Cyclic voltammetry was measured on a CHI660D electrochemical workstation in a solution of tetrabutylammonium hexafluorophosphate (Bu_4NPF_6, 0.1 M) in acetonitrile at a scan rate of 100 mV/s. The three-electrode system was composed of a glass carbon electrode coated with the sample film

as the working electrode, a Pt wire as the counter electrode, and a saturated calomel electrode (SCE) as the reference electrode. Ferrocene/ferrocenium (Fc/Fc^+) couple was used as an internal reference. Onset potentials are values obtained from the intersection of the two tangents drawn at the rising current and the baseline changing current of the CV curves. Atomic force microscopy (AFM) measurements were performed using a Bruker MULTIMODE8 in tapping mode under ambient conditions. Transmission electron microscope (TEM) measurements were performed using an Talos F200X G2. Polarized optical microscope (POM) measurements were performed using an BX51. Photoluminescence (PL) measurements were performed using an FluoroMax-4. The current density-voltage (J-V) characteristics were recorded with a Keithley 2400 source measure unit under AM 1.5G illumination (100 mW/cm^2) from a Newport solar simulator. A standard silicon solar cell was used to calibrate the light intensity. The external quantum efficiencies (EQE) of the OSCs were measured using a certified Newport incident photon conversion efficiency measurement system.

Hole-only or electron-only devices were fabricated using the architectures ITO/PEDOT:PSS/LCS:Y6/MoO_3/Ag for holes and ITO/ZnO/LCS:Y6/PDINO/Al for electrons. The mobility was extracted by fitting the current density−voltage curves using space charge limited current (SCLC), which is described by the equation

$$J = \frac{9}{8}\varepsilon_0\varepsilon_r\mu_h\frac{V^2}{d^3}$$

where J is the current, μ_h is the zero-filed mobility, and ε_0 and ε_r are the permittivity of free space and relative permittivity of the material, respectively. V is the effective voltage and d is the thickness of the organic layer. The effective voltage can be obtained by subtracting the built-in voltage (V_{bi}) and the voltage drop (V_s) from the substrate's series resistance from the applied voltage (V_{appl}): $V = V_{appl} - V_{bi} - V_s$. The hole and electron mobilities can be calculated from the slope of the $J^{1/2}-V$ curves.

Synthesis

All reactions were carried out in nitrogen atmosphere.

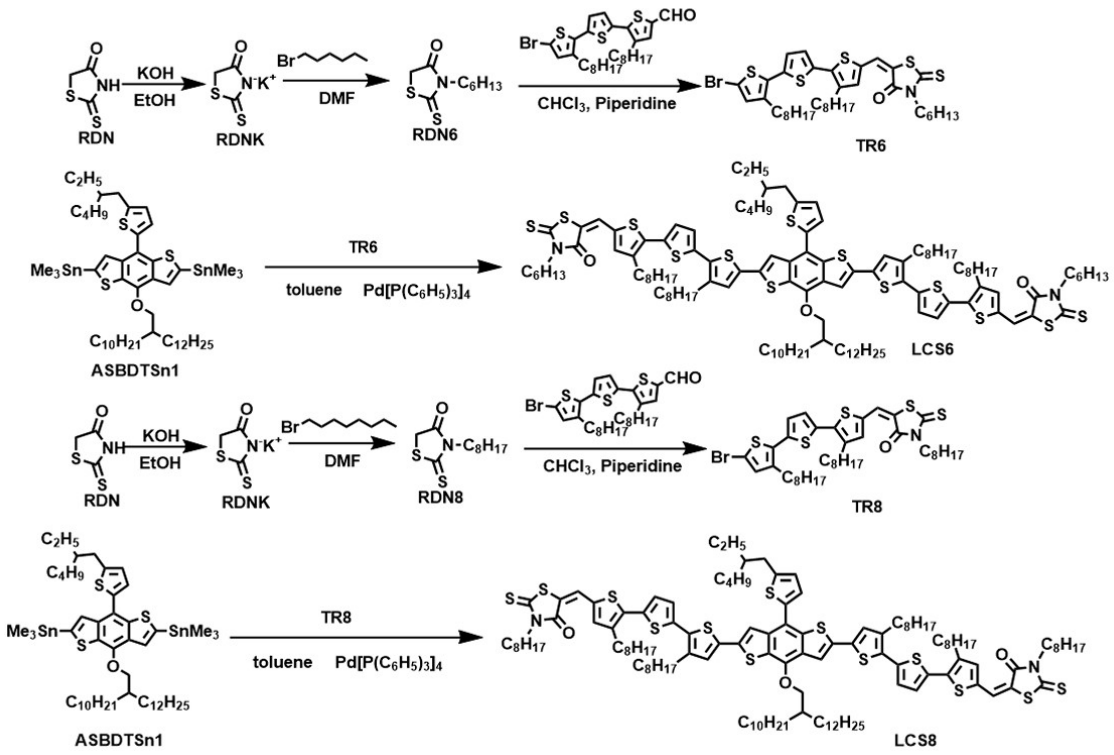

Fig. S1 Synthetic routes of LCS6 and LCS8.

(1) Synthesis of RDNK

Rhodanine (8 g, 60 mmol) and KOH (4 g, 72 mmol) were dissolved in 15 mL EtOH, respectively. Heat the rhodanine solution to 80 °C, and use a dropper funnel to add KOH solution dropwise to the rhodanine solution. The reaction mixture was kept at 80 °C for 2 hours. After stopping heating, the mixture was cooled in an ice bath for 30 minutes to precipitate a coffee colored solid. The product RDNK (7.4 g, 43 mmol, 72% yield) was obtained by filtration and rinsing with cool EtOH.

(2) Synthesis of RDN6

RDNK (7.4 g, 43.2 mmol) was added to a flask and 50 mL DMF was injected. After heating the solution to 100 °C, 1-bromohexane (7.3 mL, 51.9 mmol) was added dropwise and reacted for 12 hours. The mixture was extracted with DCM for three times. Remove the solvent to give a yellow oil (2.1 g, 10.2 mmol, 22% yield). ^{1}H NMR (600 MHz, $CDCl_3$) δ 3.99 – 3.94 (m, 4H),

1.61 (dt, J = 15.3, 7.6 Hz, 2H), 1.35 – 1.27 (m, 6H), 0.88 (t, J = 6.8 Hz, 3H).

(3) Synthesis of RDN8

RDNK (5 g, 29.2 mmol) was added to a flask and 30 mL DMF was injected. After heating the solution to 100 °C, 1-bromooctane (6.2 mL, 35 mmol) was added dropwise and reacted for 12 hours. The mixture was extracted with DCM for three times. Remove the solvent to give a yellow oil (1.3 g, 10.2 mmol, 18% yield). ^{1}H NMR (600 MHz, $CDCl_3$) δ 3.98 – 3.95 (m, 4H), 1.65 – 1.59 (m, 2H), 1.34 – 1.24 (m, 10H), 0.87 (t, J = 7.0 Hz, 3H).

(4) Synthesis of TR6

RDN6 (968 mg, 4.4 mmol） and 5-formyl-5''-bromo-3,3''-dioctyl-2,2':5',2''-trithiophene (510 mg, 0.88 mmol) were added to a flask and 10 mL $CHCl_3$ was injected. Then 0.1 mL piperidine was injected to the mixture. The mixture was stirred at room temperature for 36 hours. After removing the solvent, the residue was purified by silica gel chromatography to give a red solid (411 mg, 0.53 mmol, 60% yield). ^{1}H NMR (600 MHz, $CDCl_3$) δ 7.77 (s, 1H), 7.22 (s, 1H), 7.19 (d, J = 3.8 Hz, 1H), 7.04 (d, J = 3.8 Hz, 1H), 6.91 (s, 1H), 4.12 – 4.09 (m, 2H), 2.81 – 2.78 (m, 2H), 2.74 – 2.71 (m, 2H), 1.71 – 1.61 (m, 6H), 1.40 – 1.27 (m, 26H), 0.90 – 0.86 (m, 9H).

(5) Synthesis of TR8

RDN8 (1 g, 4.1 mmol) and 5-formyl-5''-bromo-3,3''-dioctyl-2,2':5',2''-trithiophene (475 mg, 0.82 mmol) were added to a flask and 10 mL $CHCl_3$ was injected. Then 0.1 mL piperidine was injected to the mixture. The mixture was stirred at room temperature for 36 hours. After removing the solvent, the residue was purified by silica gel chromatography to give a red solid (492 mg, 0.61 mmol, 74% yield). ^{1}H NMR (600 MHz, $CDCl_3$) δ 7.77 (s, 1H), 7.22 (s, 1H), 7.19 (d, J = 3.8 Hz, 1H), 7.04 (d, J = 3.8 Hz, 1H), 6.92 (s, 1H), 4.12 – 4.08 (m, 2H), 2.82 – 2.78 (m, 2H), 2.74 – 2.71 (m, 2H), 1.72 – 1.61 (m, 6H), 1.41 – 1.27 (m, 30H), 0.90 – 0.86 (m, 9H).

(6) Synthesis of ASBDTSn1

The compound ASBDT1 was synthesized according to the reference (*Adv.*

Mater. 2018, 30, 1705870). ASBDT1 (736 mg, 1 mmol) was added to a flask and 30 mL THF was injected. Cool down the solution to -78 °C and then add 1.6 M n-BuLi (n-hexane solution, 1.7 mL, 2.7 mmol) using a syringe and keep -78 °C for 1 hour. Subsequently, the system was slowly warmed up to room temperature, kept at room temperature for 1 hour, and then cooled down to -78 °C again. The 1 M Me_3SnCl (3.2 ml, 3.2 mmol) was injected at -78 °C and the reaction mixture was stirred at room temperature for 6 hours. 15 ml water was poured into the mixture and the mixture was extracted with DCM for three times. Remove the solvent to give a yellow liquid (950 mg, 0.9 mmol, 90% yield). ^{1}H NMR (600 MHz, $CDCl_3$) δ 7.61 (s, 1H), 7.57 (s, 1H), 7.23 (d, J = 3.6 Hz, 1H), 6.87 (d, J = 3.4 Hz, 1H), 4.27 (d, J = 5.3 Hz, 2H), 2.85 (t, J = 6.1 Hz, 2H), 1.91 – 1.86 (m, 1H), 1.70 – 1.64 (m, 3H), 1.53 – 1.27 (m, 46H), 0.96 – 0.88 (m, 12H), 0.47 – 0.37 (m, 18H).

(7) Synthesis of LCS6

TR6 (292 mg, 0.375 mmol), ASBDTSn1 (159 mg, 0.15 mmol) and $Pd(PPh_3)_4$ (30 mg) were added to a flask, then the toluene (10 mL) was injected. The reaction mixture was stirred for 48 h at 110 °C. After removing the solvent, the residue was purified by silica gel chromatography to give a black purple solid (93 mg, 0.044 mmol, 29% yield). ^{1}H NMR (600 MHz, $CDCl_3$) δ 7.76 (s, 2H), 7.57 (s, 1H), 7.50 (s, 1H), 7.25 (s, 1H), 7.22 (d, J = 3.9 Hz, 4H), 7.15 – 7.12 (m, 3H), 7.11 (s, 1H), 6.92 (d, J = 3.3 Hz, 1H), 4.26 (d, J = 5.2 Hz, 2H), 4.13 – 4.07 (m, 4H), 2.92 – 2.87 (m, 2H), 2.84 – 2.77 (m, 8H), 1.95 – 1.90 (m, 1H), 1.75 – 1.65 (m, 17H), 1.48 – 1.26 (m, 96H), 0.98 (t, J = 7.2 Hz, 3H), 0.94 (t, J = 6.7 Hz, 3H), 0.90 – 0.84 (m, 24H). ^{13}C NMR (151 MHz, $CDCl_3$) δ 192.30, 167.58, 147.66, 145.66, 141.14, 141.12, 141.08, 141.07, 139.92, 139.46, 139.43, 139.24, 137.58, 137.56, 137.31, 137.14, 136.96, 136.41, 135.67, 135.31, 135.29, 134.87, 134.84, 131.13, 130.55, 130.32, 128.42, 128.37, 128.27, 127.46, 127.30, 127.28, 126.33, 126.32, 125.49, 124.88, 120.61, 120.59, 119.48, 115.95, 76.37, 44.91, 41.53, 39.35, 34.40, 32.58, 32.00, 31.97, 31.93, 31.40, 30.58, 30.54, 30.34, 30.33, 30.25, 29.86, 29.83, 29.82, 29.78,

29.76, 29.72, 29.63, 29.61, 29.54, 29.50, 29.47, 29.46, 29.39, 29.36, 29.34, 29.33, 29.02, 27.12, 27.00, 26.51, 25.88, 23.13, 22.75, 22.73, 22.57, 14.29, 14.18, 14.17, 14.07, 11.04.

(8) Synthesis of LCS8

TR8 (302 mg, 0.375 mmol), ASBDTSn1 (159 mg, 0.15 mmol) and $Pd(PPh_3)_4$ (35 mg) were added to a flask, then the toluene (10 mL) was injected. The reaction mixture was stirred for 48 h at 110 °C. After removing the solvent, the residue was purified by silica gel chromatography to give a black purple solid (102 mg, 0.047 mmol, 31% yield). ^{1}H NMR (600 MHz, $CDCl_3$) δ 7.75 (s, 2H), 7.56 (s, 1H), 7.49 (s, 1H), 7.25 (s, 1H), 7.21 (d, J = 3.5 Hz, 4H), 7.13 (s, 3H), 7.10 (s, 1H), 6.92 (d, J = 2.8 Hz, 1H), 4.26 (d, J = 4.8 Hz, 2H), 4.12 – 4.07 (m, 4H), 2.92 – 2.87 (m, 2H), 2.84 – 2.77 (m, 8H), 1.95 – 1.89 (m, 1H), 1.76 – 1.64 (m, 17H), 1.49 – 1.26 (m, 104H), 0.99 (t, J = 7.3 Hz, 3H), 0.95 (s, 3H), 0.90 – 0.84 (m, 24H). ^{13}C NMR (151 MHz, $CDCl_3$) δ 192.28, 167.57, 147.64, 145.63, 141.10, 141.09, 141.04, 141.03, 139.90, 139.46, 139.43, 139.22, 137.57, 137.55, 137.29, 137.13, 136.96, 136.38, 135.65, 135.29, 135.27, 134.85, 134.83, 131.12, 130.55, 130.33, 128.40, 128.36, 128.25, 127.46, 127.28, 127.25, 126.30, 126.28, 125.48, 124.86, 120.59, 120.57, 119.46, 115.93, 76.35, 44.90, 41.53, 39.35, 34.40, 32.58, 31.99, 31.97, 31.93, 31.83, 31.38, 30.57, 30.53, 30.33, 30.31, 30.25, 29.86, 29.83, 29.82, 29.78, 29.75, 29.73, 29.63, 29.62, 29.54, 29.49, 29.47, 29.45, 29.39, 29.36, 29.34, 29.33, 29.19, 29.02, 27.12, 27.03, 26.85, 25.88, 23.13, 22.75, 22.73, 22.69, 14.29, 14.18, 14.17, 14.14, 11.04.

Fig. S2 ^{1}H NMR spectrum of LCS6.

Fig. S3 ^{1}H NMR spectrum of LCS8.

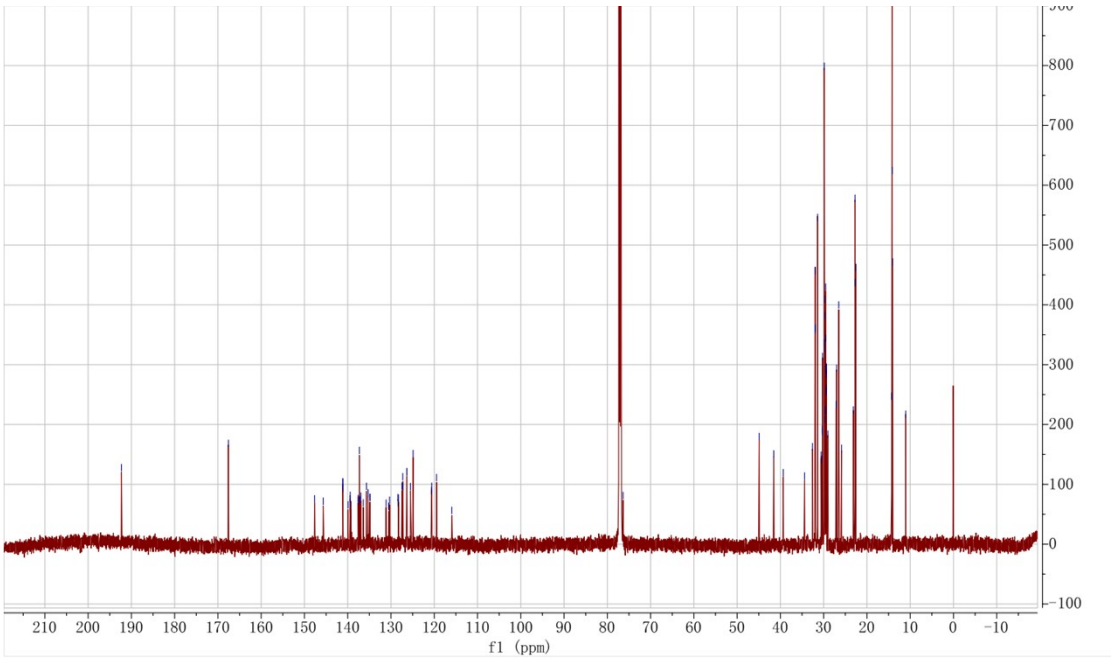

Fig. S4 ^{13}C NMR spectrum of LCS6.

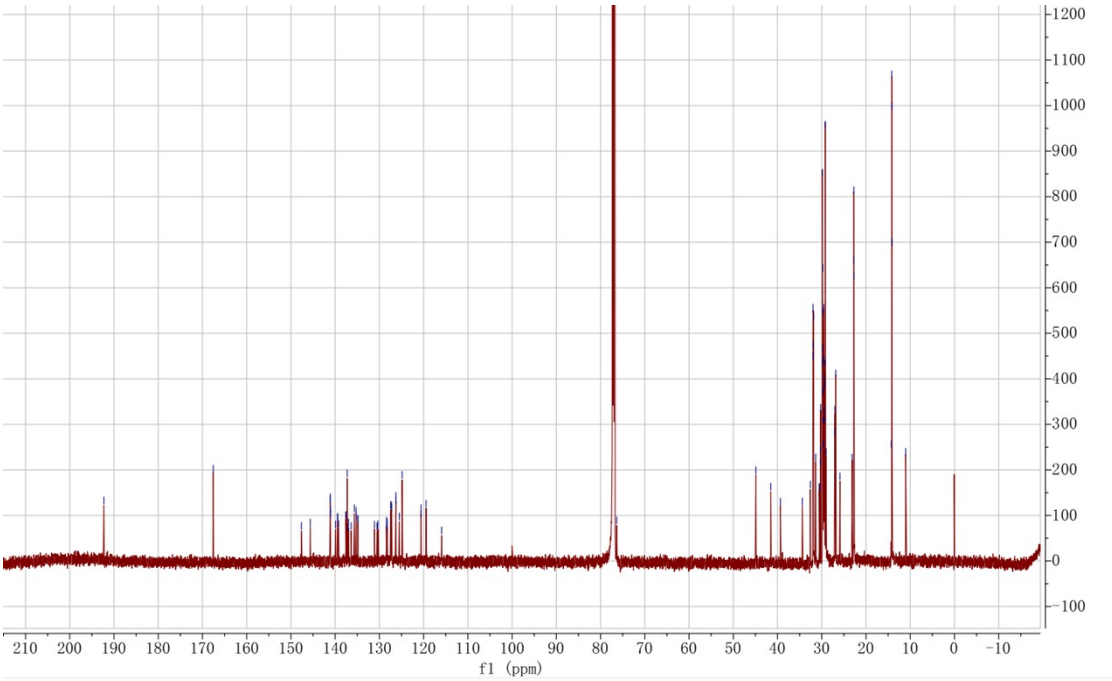

Fig. S5 ^{13}C NMR spectrum of LCS8.

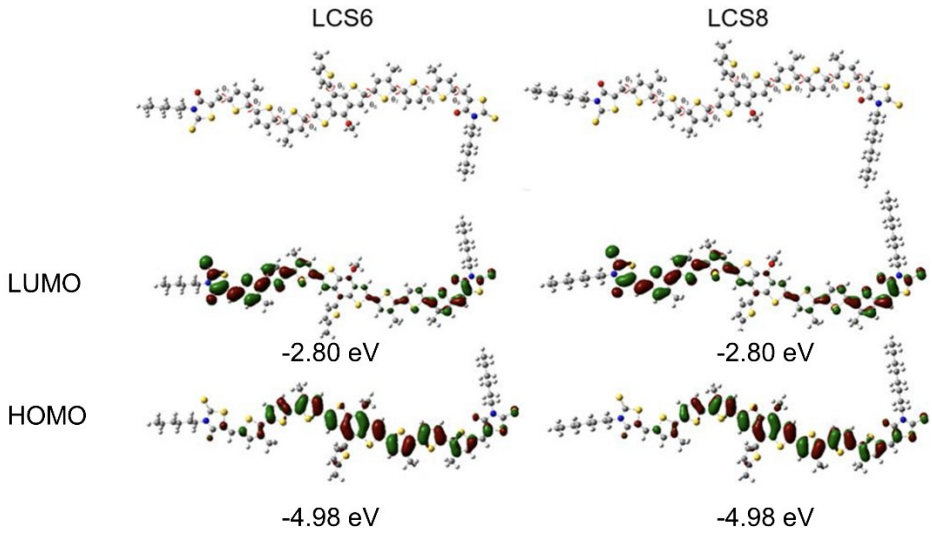

Fig. S6 Molecular configuration and HOMO and LUMO of LCS6 and LCS8 calculated by DFT at the B3LYP/6-31 (d, p) level. Gray: carbon atom, white: hydrogen atom, yellow: sulfur atom, red: oxygen atom, blue: nitrogen atom.

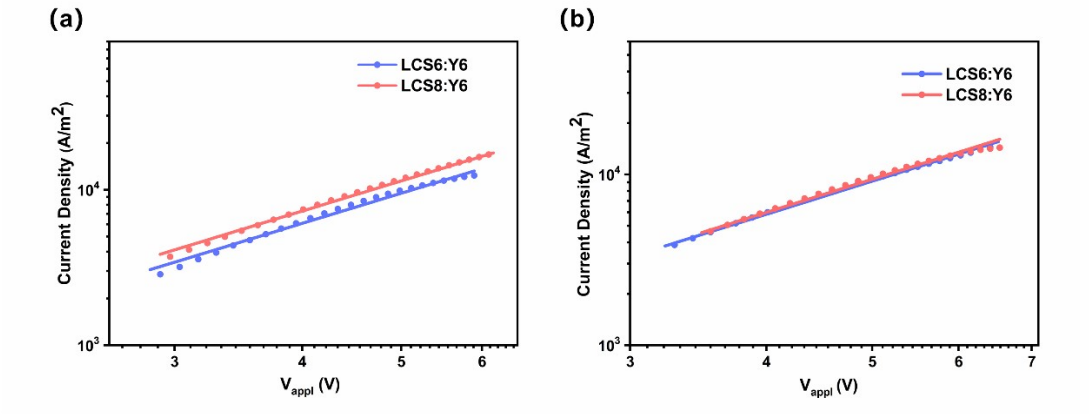

Fig. S7 Electron mobility of LCS6: Y6 and LCS8: Y6 devices (a); Hole mobility of LCS6: Y6 and LCS8: Y6 devices (b).

Table S1 Hole mobilities and electron mobilities of active layers of optimized LCS6:Y6 and LCS8:Y6 based devices.

Devices	$\mu_h \times 10^{-4}$ ($cm^2\ V^{-1}s^{-1}$)	$\mu_e \times 10^{-4}$ ($cm^2\ V^{-1}s^{-1}$)	μ_e/μ_h
LCS6:Y6	1.22	1.27	1.04
LCS8:Y6	1.25	1.53	1.22

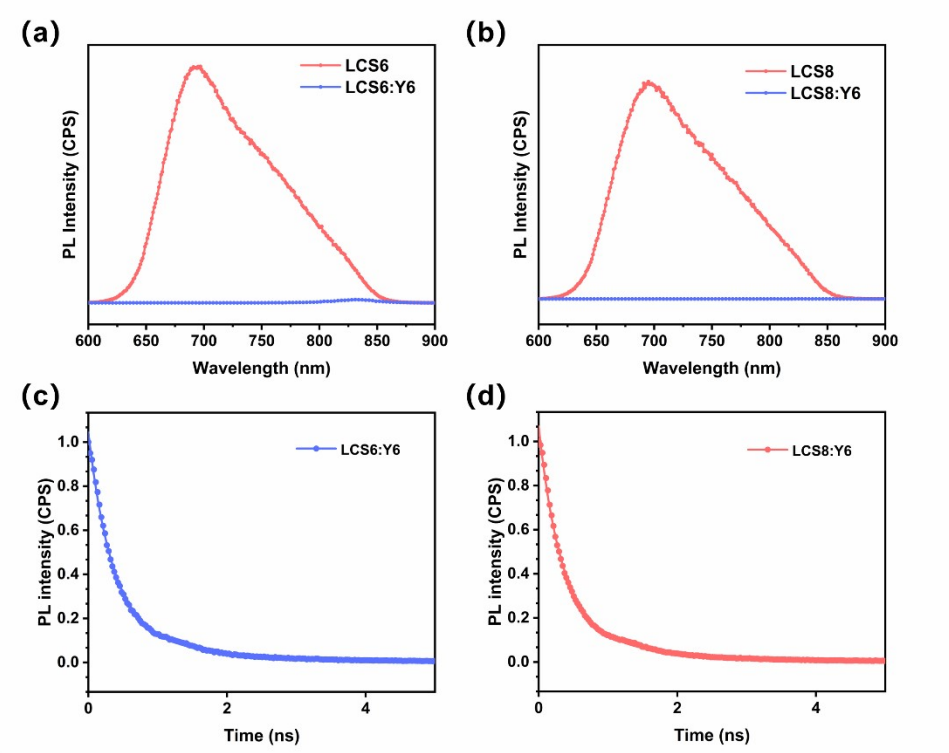

Fig. S8 Photoluminescence (PL) emission spectra of LCS6 (a)neat film and LCS6:Y6 blend film excited at 500 nm and LCS8 (b) neat film and LCS8:Y6 blend film excited at 500 nm under optimized conditions. Time-resolved photoluminescence (TRPL) emission spectra of blend films based on LCS6:Y6 (c) and LCS8:Y6 (d) under optimized condition.

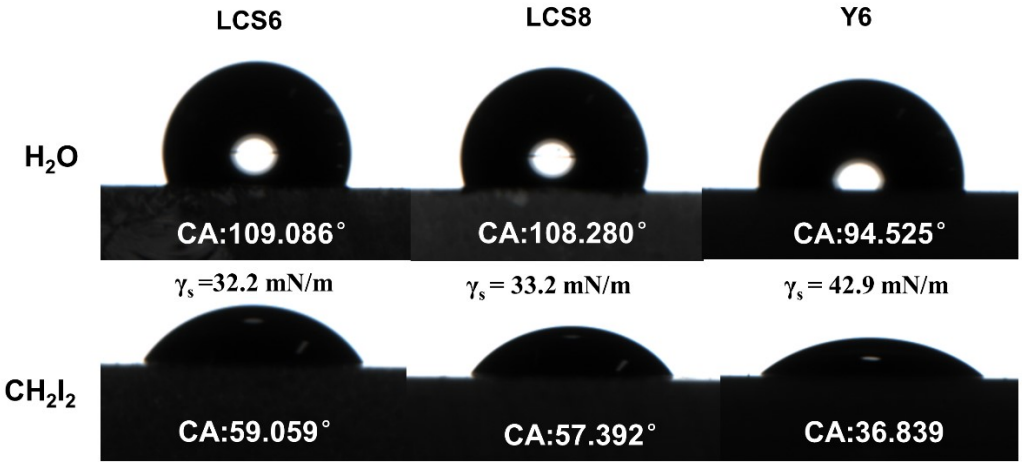

Fig. S9 Contact angle and surface energy testing for LCS6, LCS8 and Y6.

Table S2 Contact angle and surface energy testing for LCS6, LCS8 and Y6.

Materials	H_2O (°)	CH_2I_2 (°)	γ (mN/m)	χ with Y6[a]
LCS6	109.086	59.059	32.2	0.60 K
LCS8	108.280	57.392	33.2	0.47 K
Y6	94.525	36.839	42.9	/

[a] The Flory-Huggins interaction parameter (χ) was calculated from the formula, $\chi_{D,A}$ = K ($\sqrt{\gamma_D} - \sqrt{\gamma_A})^2$

Table S3 Photovoltaic performance of LCS6:Y6 devices under different donor-acceptor ratios (TA 130 °C).

D:A (w/w)	V_{OC} (V)	J_{SC} (mA/cm^2)	FF (%)	PCE (%)
0.7:1	0.79	19.03	48.37	7.29
1.1:1	**0.81**	**21.21**	**49.21**	**8.46**
1.2:1	0.80	21.46	48.26	8.32
1.3:1	0.79	23.75	43.48	8.19

Table S4 Photovoltaic performance of LCS6:Y6 devices under different annealing temperatures (D:A=1.1:1).

TA (°C)	V_{OC} (V)	J_{SC} (mA/cm^2)	FF (%)	PCE (%)
RT	0.60	1.42	24.80	0.21
80	0.86	2.77	26.47	0.63
100	0.84	17.93	43.32	6.54
130	**0.81**	**21.21**	**49.21**	**8.46**
140	0.81	19.70	51.39	8.20
150	0.70	11.93	34.09	2.86
160	0.80	10.90	47.60	4.16

Table S5 Photovoltaic performance of LCS6:Y6 devices at different annealing time (TA 130 °C).

TA time (min)	V_{OC} (V)	J_{SC} (mA/cm^2)	FF (%)	PCE (%)
7	0.80	20.13	50.79	8.23
10	0.81	21.21	49.21	8.46
13	**0.81**	**21.79**	**52.35**	**9.18**
15	0.81	21.60	50.14	8.79

Table S6 Photovoltaic performance of LCS8:Y6 devices under different donor-acceptor ratios (TA 130 °C).

D:A (w/w)	V_{OC} (V)	J_{SC} (mA/cm^2)	FF (%)	PCE (%)
0.7:1	0.80	21.86	50.71	8.90
1:1	0.80	18.13	50.28	7.26
1.3:1	**0.82**	**22.21**	**49.75**	**9.01**

Table S7 Photovoltaic performance of LCS8:Y6 devices under different annealing temperatures (D:A=1.3:1).

TA (°C)	V_{OC} (V)	J_{SC} (mA/cm^2)	FF (%)	PCE (%)
RT	0.42	0.75	24.26	0.08
80	0.57	2.53	25.29	0.36
110	0.81	22.02	49.67	8.82
120	0.81	21.43	47.84	8.30
130	**0.82**	**22.21**	**49.75**	**9.01**
140	0.82	21.47	47.87	8.41

Table S8 Photovoltaic performance of LCS8:Y6 devices at different annealing time (TA 130 °C).

TA time (min)	V_{OC} (V)	J_{SC} (mA/cm^2)	FF (%)	PCE (%)
10	0.82	22.21	49.75	9.01
13	**0.82**	**20.68**	**54.00**	**9.15**
15	0.82	19.77	54.88	8.86